A&A manuscript no.
(will be inserted by hand later)

Your thesaurus codes are:
06 (08.02.4, 08.05.1, 08.06.3, 10.11.1, 10.15.1, 10.15.2 (Bochum 2))

ASTRONOMY
AND
ASTROPHYSICS
2.12.1998

Kinematics and binaries in young stellar aggregates. I. The trapezium system BD+00°1617 in Bochum 2*

Ulisse Munari[1] **and Lina Tomasella**[2]

[1] Osservatorio Astronomico di Padova, Sede di Asiago, I-36012 Asiago (VI), Italy (munari@pd.astro.it)
[2] Osservatorio Astrofisico del Dip. di Astronomia, Università di Padova, I-36012 Asiago (VI), Italy (tomasella@pd.astro.it)

Received date.............; accepted date................

Abstract. Internal kinematics, spectroscopic binaries and galactic motion are investigated for the trapezium system BD+00°1617 (which lies at the heart of the young open cluster Bochum 2) by means on 73 high resolution Echelle+CCD spectra secured over the period 1994-98. Two of the three O-type member stars are found to be binaries on close and highly eccentric orbits of 6.8 and 11.0 day period. The spectra of the two binaries show large variations in the half-intensity and equivalent widths of the HeI absorption lines, which are intrinsic to the primaries and are not correlated to the orbital phase. Astrometric and radial velocities exclude that one of the component is leaving as a runaway star, but upper limits are still compatible with the trapezium evaporating at very low relative velocities. The projected rotational velocities of the three constituent O–type stars are low. This conforms to expectations from the high frequency of binaries. The observed radial velocity of Bochum 2 agrees with the Hron (1987) expression for the Galaxy rotation inside the latter's quoted errors.

Key words: Binaries: spectroscopic – Stars: early type – Stars: fundamental parameters – Galaxy: kinematics and dynamics – Open clusters and associations: individual (Bochum 2)

1. Introduction

With this paper we begin a series devoted to the results of a prolonged high resolution spectroscopic monitoring of early type members of young open clusters, trapezium systems and OB associations. The emphasis is on accurate and extensive radial velocities (secured over several years), suitable to trace (*a*) the internal kinematics, (*b*) the galactic motion, (*c*) the binary star content and the spectroscopic orbits. The high dispersion spectra are also useful to derive the projected rotational velocities, the chemical composition and the evolutionary status of the member stars as well as to study the interstellar medium inside and towards such young stellar aggregates. These latter aspects are however broadly outside the scope of the present series and will be considered elsewhere.

Our program encompasses a selection of young stellar aggregates spanning a range in total mass, number of member stars, age, total energy, etc. The targets have been chosen, whenever possible, among those with already published high quality astrometry and photometry. We believe that much can be learned by extensive and homogeneous high–res spectral campaign data on such targets and to this aim we begun in 1990 a long term program with the telescopes and spectrographs of the Asiago Astrophysical Observatory. The ambitious goal is to search for *observationally* proved grand-relations governing the dynamical evolution of the young stellar aggregates which could then be compared with the predictions of N-body simulations. Such grand-relations are expected to become apparent when a significant number of young stellar aggregates will have been studied in the most homogeneous way and for such a reason we will postpone later in the present series a throughout discussion of the results accumulated on the way.

We start with a so far poorly studied trapezium system (BD+00°1617) at the heart of a dim and very young open cluster (Bochum 2), which lies at a great distance in the general anti–center galactic direction (at $\sim$ 14 kpc galacto-centric distance).

Trapezium systems are groups of three or more stars whose apparent separations onto the sky are similar, as for the prototype of the class, the four O stars at the core of the Orion open cluster and nebula. OB associations contain typically three to five trapezia and these configurations have a high frequency among T-associations too. Within stellar associations, trapezia appear to cluster close to the nuclei of open clusters and emission nebulae. A trapezium-like configuration is in general dynamically unstable and therefore it must be young. It has to evolve either into (*a*) *hierarchical systems* (i.e. ones in which the separation of successive binaries increases by large factors;

Send offprint requests to: U.Munari

* Tables 2 and 3 are only available in electronic form at the CDS via anonymous ftp to cdsarc.u-strasbg.fr (130.79.128.5) or via http://cdsweb.u-strasbg.fr/Abstract.html

they are dynamically stable and are present among systems of all ages), or into (*b*) *hard binaries* (with possible ejection from the system of one or more of the trapezium components). Ambartsumian (1954) computed in $1 \div 2 \times 10^4$ AU the largest stable dimension of a trapezium in the solar vicinity against perturbation by passing stars: the one order of magnitude larger extension (1×10^5 AU) for cataloged trapezia reinforces the notion that they must be dynamically young systems. The first catalog of trapezium systems has been compiled by Ambartsumian (1954), listing 108 entries and a more recent one (442 systems) has been presented by Salukvadze (1978). Trapezia have been traditionally found by filtering catalogs of visual binaries, like the Index Catalog of Visual Binary Stars (IDS) by Jeffers et al. (1963).

Bochum 2 ($\alpha_{2000} = 06^h49^m$, $\delta_{2000} = +00°23'$, $l = 212.3$, $b = -0.4$) has been studied by Moffat & Vogt (1975), Turbide & Moffat (1993) and Munari & Carraro (1995, hereafter MC95). At its center lies BD+00°1617*A*-*B*-*C*, a system of three O-type stars which luminosity largely dominates the apparently dim surrounding cluster. The three O stars are plotted in the finding chart of Figure 1. They appear equally spaced and on a straight line in the projection onto the sky.

Bochum 2 is not included in catalogs of trapezium systems most probably because BD+00°1617*A*-*B*-*C* is oddly missing from catalogs of visual binaries. However, it fully satisfies all classification criteria and in the following it will be discussed as a validated trapezium system. The three components will be identified in the following according to the numbering by MC95 (#20, #21 and #23, cf. Figure 1).

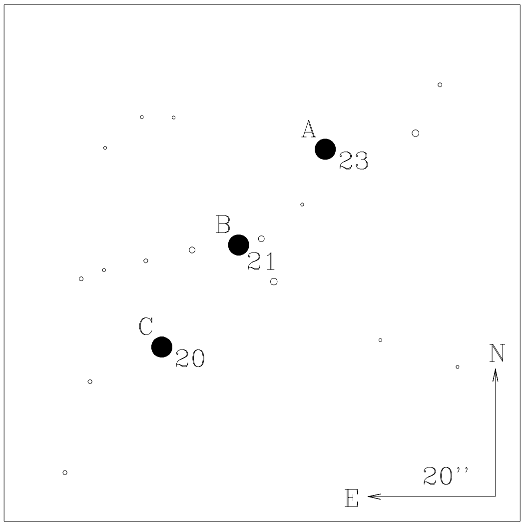

Fig. 1. Finding chart for the program trapezium stars at the heart of the open cluster Bochum 2. Orientation and scale are given. Capital letters relates to BD+00°1617 sub-classification, the numbers to the identification in Munari & Carraro (1995).

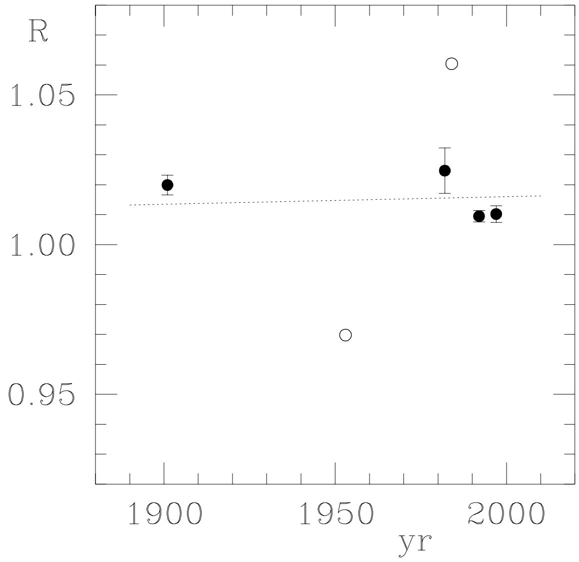

Fig. 2. Change with time of the distance between stars *A* and *B* compared to that between stars *B* and *C* [R = $\triangle(\overline{AB}/\overline{BC})$]. The dashed line is a last square fit and the error bars are 3σ values. Solid circles are from the Astrographic Catalogue, the USNO Twin Astrographic Catalogue and some recent CCD observations, the open circles from Palomar Schmidt POSS-I (USNO A1.0 Catalogue) and GSC-I.

2. Observations

The program stars are listed in Table 1. Photometric and spectroscopic data come from MC95. Positions are from the *Astrographic Catalog* for the epoch 1901.0 and equinox J2000.0 (see section 2.2), placed on the reference system of the Hipparcos Catalogue. The journal of the observations is given in Table 2.

2.1. Spectroscopy

Seventy-three high resolution spectra of the program stars have been secured from Nov. 1994 to Feb. 1998 with the 1.82 m telescope and Echelle+CCD spectrograph of the Astronomical Observatory of Padova at Asiago (Cima Ekar). The wavelength range covered on a single frame was generally from Hδ to HeI 6678 Å, with some spectra extending up to 9900 Å and a few others down to 3865 Å (cf. Table 2 for details). The instrumental PSF (from the FWHM of night-sky lines and thorium lines in the comparison spectra) is generally uniform over the various order and pretty constant during the 5 years of observations, corresponding to an average of 14 km sec^{-1} for full resolution frames and to 20 km sec^{-1} for those with a 2×2 binning (corresponding respectively to 0.22 and 0.32 Å resolution at Hβ). Details on the instrument, its performances and the use are given in Munari & Zwitter (1994).

Table 1. Program stars. Identification numbers, photometry and spectroscopy from Munari & Carraro (1995; MC95), positions from the Astrographic Catalog 2000 reduced to the Hipparcos Catalogue reference system.

MC95 #	BD	LS	GSC #	*V*	*U-B*	*B-V*	spectrum	α_{J2000} (epoch 1901.0)	δ_{J2000} (epoch 1901.0)
20	+00°1617 C	VI +00 26	1481994	11.21	–0.52	0.49	O9 V	$06^h\,48^m\,51.^s300$	$+00^\circ\,22'\,21.''49$
21	+00°1617 B	VI +00 25	1482125	11.01	–0.48	0.53	O7 V	$06^h\,48^m\,50.^s484$	$+00^\circ\,22'\,37.''62$
23	+00°1617 A	VI +00 24	1481965	11.38	–0.52	0.51	O9 V	$06^h\,48^m\,49.^s541$	$+00^\circ\,22'\,52.''71$

Table 2. Journal of observations. *N* = spectrum number from the telescope logbook; # = program star identification number; *HJD* = heliocentric JD - 2400000; *Res: f* = full-resolution spectrum, *b* = 2 × 2 binned spectrum; *S/N* = signal-to-noise ratio for the stellar continuum close to the NaI D doublet (center of Echelle order 38), or center of order 26 for last entries. Column *Orders* lists the Echelle spectral orders covered on the given spectrum, which corresponds to the following wavelength ranges: *23-29* = 9900–7600 Å, *28-38* = 8130–5800 Å, *29-41* = 7850–5375 Å, *33-51* = 6900–4320 Å, *33-52* = 6900–4240 Å, *34-51* = 6695–4320 Å, *34-50* = 6695–4410 Å, *34-53* = 6695–4160 Å, *37-50* = 6150–4410 Å, *38-57* = 5990–3865 Å, *39-58* = 5835–3800 Å. The HJD of the last three spectra is the same because their spectra have been recorded simultaneously on the same CCD frame.

N	#	Date	HJD	Res.	Orders	S/N	N	#	Date	HJD	Res.	Orders	S/N
17522	21	13.11.94	49669.554	f	38–57	29	23901	21	22.02.97	50502.365	b	34–53	49
17524	20	13.11.94	49669.584	f	38–57	26	23903	20	22.02.97	50502.389	b	34–53	50
17526	23	13.11.94	49669.622	f	38–57	27	24457	21	25.03.97	50533.367	b	34–53	21
17869	21	16.12.94	49703.411	f	29–41	33	24459	20	25.03.97	50533.384	b	34–53	18
17871	20	16.12.94	49703.438	f	29–41	35	24461	21	25.03.97	50533.400	b	34–51	17
17873	23	16.12.94	49703.472	f	29–41	32	24477	21	27.03.97	50535.266	b	34–53	32
18336	21	15.01.95	49733.379	f	34–53	39	24479	20	27.03.97	50535.278	b	34–53	35
18337	20	15.01.95	49733.410	f	34–53	48	24483	21	27.03.97	50535.306	b	34–53	21
18339	23	15.01.95	49733.457	f	34–53	47	24485	20	27.03.97	50535.322	b	34–53	32
21191	23	10.12.95	50061.650	b	34–53	33	24487	23	27.03.97	50535.346	b	34–53	36
21237	23	11.12.95	50062.589	b	34–53	38	24489	21	27.03.97	50535.369	b	34–53	28
21239	21	11.12.95	50062.602	b	34–53	39	24491	20	27.03.97	50535.386	b	34–53	24
21241	20	11.12.95	50062.616	b	34–53	29	24651	20	16.04.97	50555.282	b	34–50	16
21276	23	12.12.95	50063.558	b	34–53	32	24653	21	16.04.97	50555.295	b	34–53	34
21595	23	31.03.96	50174.372	b	34–53	18	24655	20	16.04.97	50555.312	b	34–53	31
21597	21	31.03.96	50174.389	b	34–53	15	24699	20	17.04.97	50556.297	b	34–53	45
21696	20	06.04.96	50180.314	b	34–53	29	24701	21	17.04.97	50556.315	b	34–53	49
21698	20	06.04.96	50180.334	b	34–53	23	24703	23	17.04.97	50556.332	b	34–53	48
21700	21	06.04.96	50180.368	b	34–53	26	24770	20	18.04.97	50557.290	b	34–53	39
22588	23	30.12.96	50447.578	b	33–52	41	24772	21	18.04.97	50557.313	b	34–53	42
22590	21	30.12.96	50447.591	b	33–52	57	24774	20	18.04.97	50557.332	b	34–53	26
22592	20	30.12.96	50447.607	b	33–52	35	26468	20	14.11.97	50766.603	b	34–53	38
23061	20	27.01.97	50475.501	b	34–53	30	26472	21	14.11.97	50766.650	b	34–53	45
23063	21	27.01.97	50475.514	b	34–53	34	26474	20	14.11.97	50766.673	b	34–53	42
23065	23	27.01.97	50475.527	b	34–53	26	26506	20	15.11.97	50767.595	b	34–53	30
23168	20	28.01.97	50476.505	b	34–53	23	26510	21	15.11.97	50767.637	b	34–53	32
23170	21	28.01.97	50476.521	b	34–51	24	26512	20	15.11.97	50767.661	b	34–53	25
23172	23	28.01.97	50476.538	b	34–51	19	26518	20	15.11.97	50767.700	b	34–53	25
23644	20	17.02.97	50497.358	b	33–51	32	27068	20	13.12.97	50795.522	b	28–38	24
23645	21	17.02.97	50497.381	b	33–51	36	27070	21	13.12.97	50795.546	b	28–38	31
23647	23	17.02.97	50497.404	b	33–51	36	27471	20	11.01.98	50825.461	b	39–58	54
23723	23	18.02.97	50498.353	f	33–50	23	27473	21	11.01.98	50825.485	b	39–58	83
23725	21	18.02.97	50498.401	f	33–50	16	27474	20	12.01.98	50825.515	b	39–58	72
23823	21	21.02.97	50501.342	f	34–53	38	27653	20	05.02.98	50850.450	b	23–29	45
23825	20	21.02.97	50501.390	f	34–53	36	27653	21	05.02.98	50850.450	b	23–29	60
23827	23	21.02.97	50501.437	f	34–53	29	27653	23	05.02.98	50850.450	b	23–29	38
23899	23	22.02.97	50502.330	f	34–53	40							

Table 3. Heliocentric radial velocities and associated errors for the three program stars. *N*°= spectrum number as in Table 2.

#20				#21				#23			
N	HJD	$RV_\odot$	err.	N	HJD	$RV_\odot$	err.	N	HJD	$RV_\odot$	err.
17524	49669.584	54.7	1.3	17522	49669.554	83.8	1.2	17526	49669.622	68.1	2.9
17871	49703.438	56.0	0.4	17869	49703.411	54.7	2.7	17873	49703.472	68.3	0.3
18337	49733.410	44.0	1.1	18336	49733.379	133.7	1.5	18339	49733.457	69.2	2.2
21241	50062.616	48.9	1.4	21239	50062.602	71.4	1.3	21191	50061.650	65.5	3.6
21696	50180.314	101.5	2.9	21597	50174.389	135.2	1.5	21237	50062.589	67.0	1.0
21698	50180.334	113.4	0.4	21700	50180.368	7.3	2.0	21276	50063.558	68.5	1.1
22592	50447.607	103.9	1.7	22590	50447.591	34.2	2.5	21595	50174.372	65.8	3.6
23061	50475.501	107.3	0.8	23063	50475.514	46.9	0.7	22588	50447.578	67.6	1.9
23168	50476.505	89.3	6.0	23170	50476.521	47.5	5.4	23065	50475.527	68.0	3.0
23644	50497.358	78.5	0.9	23645	50497.381	69.9	0.7	23172	50476.538	70.3	5.5
23825	50501.390	46.7	1.4	23725	50498.401	51.3	1.1	23647	50497.404	69.2	1.3
23903	50502.389	85.1	1.8	23823	50501.342	15.8	1.9	23723	50498.353	67.7	2.5
24459	50533.384	47.5	0.9	23901	50502.365	22.1	1.1	23827	50501.437	67.8	2.2
24479	50535.278	44.8	0.8	24457	50533.367	3.4	3.6	23899	50502.330	71.5	2.7
24485	50535.322	44.3	3.2	24461	50533.400	5.2	3.8	24487	50535.346	69.2	1.0
24491	50535.386	50.2	1.2	24477	50535.266	13.5	3.5	24703	50556.332	68.8	2.1
24651	50555.282	50.7	0.4	24483	50535.306	20.7	2.5	27553	50850.450	69.0	7.0
24655	50555.312	48.0	0.8	24489	50535.369	6.0	3.6				
24699	50556.297	51.7	4.9	24653	50555.295	13.0	2.2				
24770	50557.290	106.4	0.8	24701	50556.315	8.9	5.0				
24774	50557.332	97.3	0.4	24772	50557.313	17.9	1.1				
26468	50766.603	50.3	6.0	26472	50766.650	12.5	3.9				
26474	50766.673	53.7	2.9	26510	50767.637	39.0	4.6				
26506	50767.595	52.8	1.1	27070	50795.546	51.0	2.4				
26512	50767.661	50.9	4.7	27473	50825.485	138.9	2.0				
26518	50767.700	47.7	3.1	27553	50850.450	51.9	5.1				
27068	50795.522	48.9	7.4								
27471	50825.461	115.5	15.0								
27474	50825.515	110.8	1.5								
27553	50850.450	49.9	8.0								

Table 4. Orbital elements for stars #20 and #21. The last row gives the weighted deviation of the observed radial velocities from the computed orbital solution. The quoted errors are the formal errors of the orbital solution. *HJD* = heliocentric JD – 2400000.

		#20		#21	
period	(days)	6.858	±0.004	11.030	±0.006
baricentric velocity	(km sec^{-1})	69.8	± 1.5	63.0	± 1.6
semi-amplitude	(km sec^{-1})	33.3	± 2.3	64.9	± 2.6
eccentricity		0.43	± 0.17	0.21	± 0.05
$a \sin i$	(AU)	0.0019	± 0.0001	0.065	± 0.003
$T_\circ$	(HJD)	50831.786	± 0.278	50835.749	± 0.434
Ω	(deg)	316	± 19	322	± 14
mass function		0.019		0.29	
deviation	(km sec^{-1})	4.2		4.8	

Table 5. Dispersion (σ), mean and error of the mean for equivalent widths (EW) and half-intensity widths (HIW) of λ 5876 Å HeI line. The projected rotational velocities are from Equation (8).

#	EW (Å)		HIW (Å)		V_{rot} sin$i$
	σ	mean	σ	mean	(km sec^{-1})
20	0.20	0.73±0.04	0.53	3.01±0.13	92±8
21	0.11	0.60±0.03	0.62	3.14±0.14	98±9
23	0.010	0.706±0.003	0.07	1.54±0.02	30±5

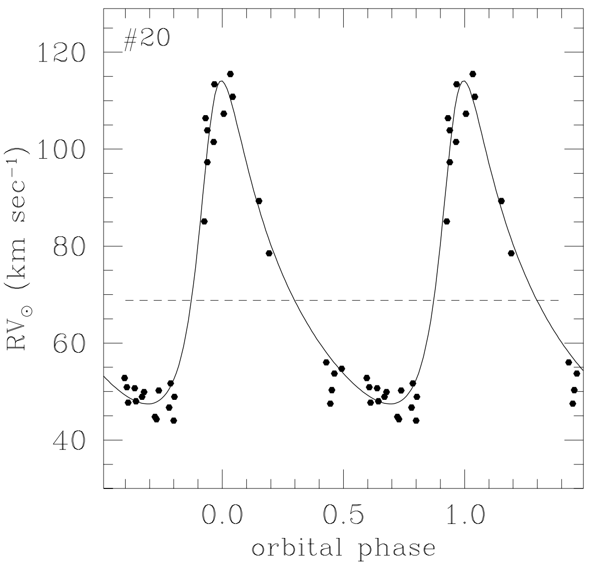

Fig. 3. Orbital solution for star #20. The solid line refers to the orbital solution given in Table 4. The dashed line is the baricentric velocity (69.8 km sec^{-1}).

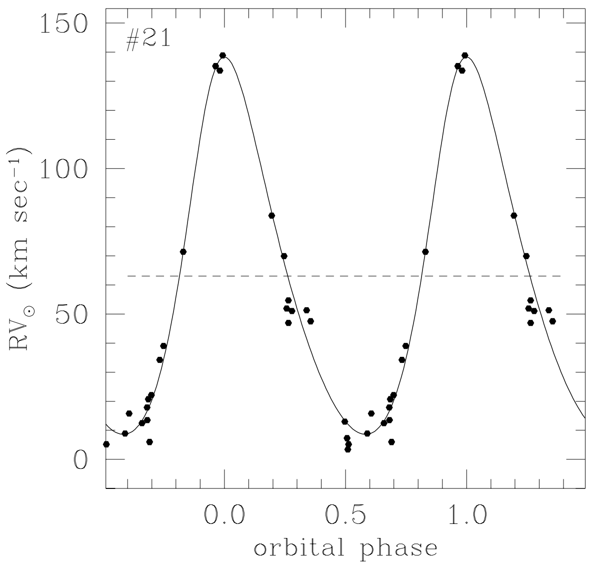

Fig. 4. Orbital solution for star #21. The solid line refers to the orbital solution given in Table 4. The dashed line is the baricentric velocity (63.0 km sec^{-1}).

The spectra have been extracted and calibrated in a standard fashion using the IRAF reduction package. Great care has been taken to ensure the highest quality in the wavelength calibration and therefore its suitability for accurate radial velocity measurements. The flexure pattern of the Asiago spectrographs (and their negligible influence on derivation of accurate RVs) has been studied in detail by Munari & Lattanzi (1992). The small (however always smooth and predictable) flexures induced by telescope tracking on the targets has been removed accordingly.

Some checks have been performed to control the accuracy of the wavelength scale of the calibrated 1-D spectra. A brief description of the results from these checks follows.

(*i*) At the S/N ratios given in Table 2 only a few of the strongest telluric absorption lines are detectable on a single spectrum. Therefore, for each program star we have summed up in the velocity space all wavelength calibrated 1-D spectra. On the summed-up spectra many telluric lines (as weak as to produce an equivalent width of only 0.004 Å) are measurable. Their mean radial velocity has turned out to be 0.0 km sec^{-1} with a dispersion of 0.52 km sec^{-1}, largely dominated by the difficulty to measure so weak features. This supports the conclusion by Munari & Lattanzi (1992) that the Asiago Echelle+CCD spectrograph has a completely negligible (if any) *spectrograph velocity* or systematic offset.

(*ii*) Our spectra have been exposed for an average of 30 minutes and at an average height over the horizon of 38 degrees. In these condition strong night-sky lines are expected and have been indeed recorded on our spectra. On all spectra we have measured the three strongest night-sky lines, which lay on separate Echelle orders. The results confirm the high control over the wavelength calibration, with a mean radial velocity of 0.0 km sec^{-1} and a typical dispersion of 0.19 km sec^{-1} (the lower dispersion compared with the weak telluric lines has to be ascribed to the higher S/N ratio of the night-sky lines).

(*iii*) Finally, nearly all spectra cover the region of the interstellar NaI D doublet. We have measured its radial velocity,

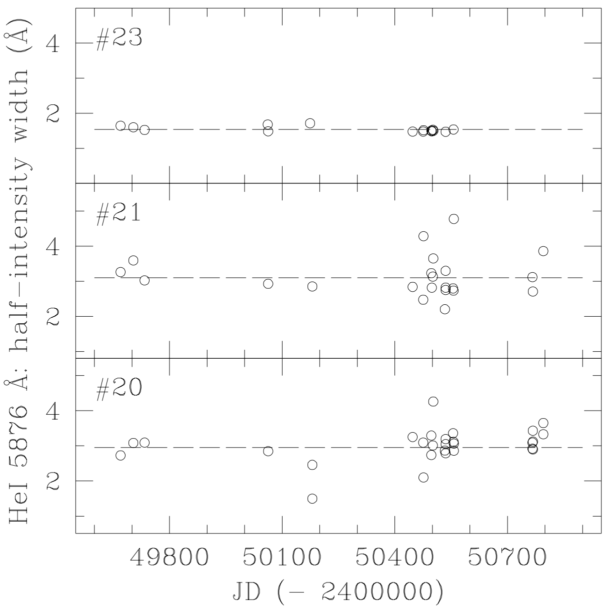

Fig. 5. Half-intensity width (Å) of λ 5876 Å HeI on spectra of programme stars #20 (upper panel), #21 (center) and #23 (lower panel). The dashed lines represent the mean values.

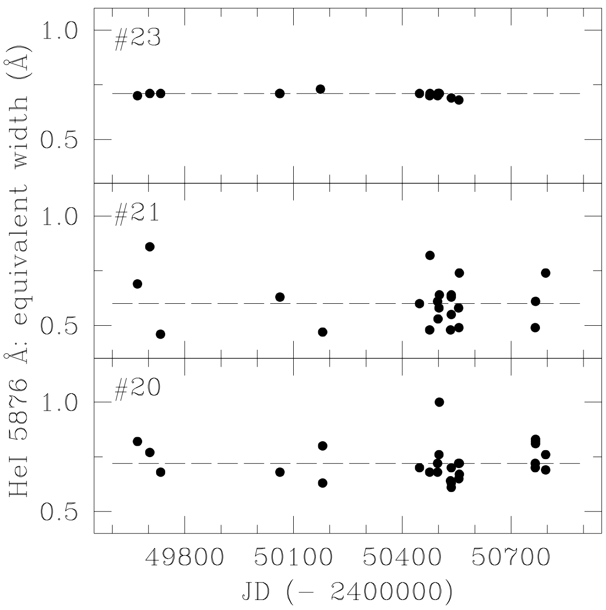

Fig. 6. Equivalent width (Å) of λ 5876 Å HeI on spectra of programme stars #20 (upper panel), #21 (center) and #23 (lower panel). The dashed lines represent the mean values.

with the following results:

$$RV_{\odot}^{NaI}(\#20) = 40.94 \pm 0.18 \quad (\sigma = 0.92) \quad km\ sec^{-1} \qquad (1)$$

$$RV_{\odot}^{NaI}(\#21) = 41.06 \pm 0.23 \quad (\sigma = 1.09) \quad km\ sec^{-1} \qquad (2)$$

$$RV_{\odot}^{NaI}(\#23) = 40.33 \pm 0.24 \quad (\sigma = 0.95) \quad km\ sec^{-1} \qquad (3)$$

where the standard error of the mean and the dispersion of the measurements are given. Again, the low values for σ confirm the accuracy and repeatability of the wavelength scale during the night and over several years.

2.2. Astrometry

Some constraints on the internal dynamics of the trapezium system BD+00°1617 can be derived from data available in published astrometric catalogues, supplemented by some recent ground-based CCD observations. BD+00°1617 was included in the first version of the Tycho Input Catalogue (TIC), but unfortunately it did not pass the Recognition Process after one year of satellite operation which led to the final version of the TIC (Halbwachs et al. 1994). Plates from the POSS-II covering the Bochum 2 area have not yet been digitized by the time this paper has been written, and so preliminary GSC-II data are not available.

The oldest epoch data for BD+00°1617 come from the *Astrographic Catalogue as reduced to the ACRS* released by the United States Naval Observatory (USNO, cf. Urban & Corbin 1994, 1996). Bochum 2 is in the zone photographed in 1901 by the Observatory of Algiers. Intermediate epoch data are available from (*a*) the 1984 Palomar Schmidt plates used for the Guide Star Catalogue (GSC-I; Lasker et al. 1990), (*b*) the astrometric reduction of the plates of the original Palomar Sky Survey (POSS-I) performed at USNO and known as the A1.0 Catalogue and, finally, (*c*) positions measured along the USNO Twin Astrographic Catalogue project (Zacharias et al. 1996).

Recent epoch astrometric data come from MC95 (the X,Y in their Table 3). Similar observations have been secured with the 1.22 m reflector of the Asiago Astrophysical Observatory during the commissioning in Feb. 1997 of a new CCD camera for the Newton focus (6 m focal length). For both MC95 and Asiago data, no field stars suitable to arrange a local astrometric reference system entered the CCD field around Bochum 2, and therefore no reduction to J2000.0 positions has been possible. Only relative positions between components *A*, *B* and *C* of BD+00°1617 have been measured. They are plotted in Figure 2 as the ratio of the distance from component *A* to *B*, with respect to distance from *B* to *C*. The same ratio has been computed for the other data sets above described and plotted in the figure.

A 3σ error bar can be derived for the Astrographic Catalogue and the CCD data, but not unambiguously for the GSC and POSS ones. The latter two appear in Figure 2 to be of poorer astrometric quality (possibly due to the blending with nearby faints stars of the associated cluster and the notoriously complicated focal field geometry of Schmidt telescopes) and will not be considered further on.

Figure 2 does not support a detectable change of the relative distances of the three program stars ($\overline{AB} \sim \overline{BC} \sim 20.''5$) over the last century. A least square solution (of quite low statistical significance) may indicate a change by ∼0.2% over the time span by the data in Figure 2 (about a century). At a distance (D) to Bochum 2 of $\sim$ 6 kpc it corresponds to a projected relative velocity of

$$V_{projected} \sim 10 \left(\frac{D}{6\ kpc}\right) \quad km\ sec^{-1} \tag{4}$$

It does not support a runaway status for any of the program stars and it is largely compatible inside the errors with a negative total energy (a gravitationally bound trapezium).

In view of the limited accuracy and overall paucity of available data, a confirmation and refinement of the astrometric results would be desiderable through a search in plates archives for suitable old and intermediate epoch astrometric plates covering the region of Bochum 2.

3. Radial Velocities

Radial velocities have been first measured on the calibrated spectra by fitting individually each absorption line (with reference wavelengths taken from Moore 1959). This soon led to the recognition of star #23 as a constant radial velocity star and the other two program stars as binaries. The heliocentric radial velocity of star #23 (cf. Table 3) has been found to be:

$$RV_{\odot}^{\#23} = 68.3 \pm 0.3 \quad (\sigma = 1.4) \quad km\ sec^{-1} \tag{5}$$

Three times the σ = 1.4 km sec^{-1} can be taken as the threshold for detection of binarity among the program stars. Using #23 as a RV standard star we have proceeded to re-evaluate radial velocities of #20 and #21 by cross-correlation (with the IRAF task *fxcor*). The results are listed in Table 3.

Taking a mean between the velocity of #23 and the baricentric velocities of #20 and #21 (see next section and Table 4), the trapezium (and hence cluster) heliocentric radial velocity is (weighted mean):

$$RV_{\odot}^{cl} = 68 \pm 3 \quad km\ sec^{-1} \tag{6}$$

To the best of our knowledge, only Jackson et al. (1979) have so far published a radial velocity determination for Bochum 2. They reported a 49 km sec^{-1} from a few spectra of one or more of our same program stars. Unfortunately they gave no further detail. A $\pm$7 km sec^{-1} error is attached to this value by Turbide & Moffat (1993). Given the large amplitude of radial velocity variation by the the program stars and the absence of informations on the number and quality of the measurements by Jackson et al. (1979), their RV for Bochum 2 will not be considered in the following.

4. Spectroscopic Orbits

The large variability of the radial velocities of #20 and #21 compared to the constancy for #23 (cf. Table 3) argues for #20 and #21 to be binaries. We have therefore proceeded with period search and determination of the spectroscopic orbits for the latter two stars.

The orbital periods of #20 and #21 turned out to be $6\overset{d}{.}858$ and $11\overset{d}{.}030$, respectively. The orbital solutions computed from these orbital periods are listed in Table 4 and in graphical form are presented in Figures 3 and 4. The errors of the orbital solutions are of the order of 5% or less. The larger errors for the eccentricities may results from the uneven distribution of the observations along the orbital phase.

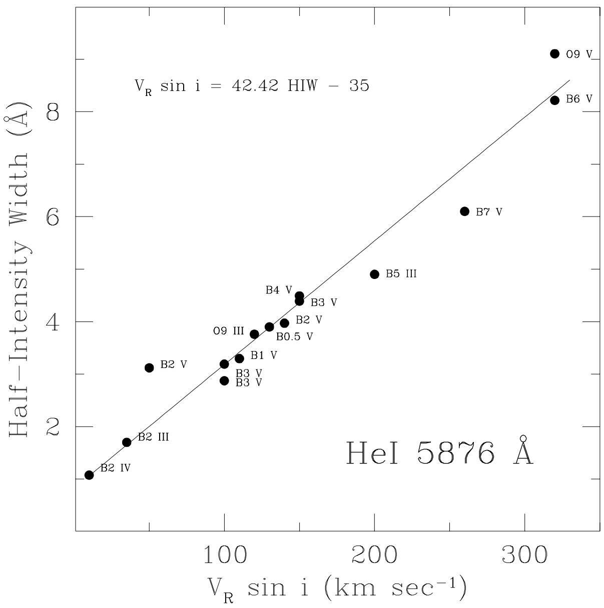

Fig. 7. Calibration for our Echelle+CCD spectrograph of the relation between half-intensity width (HIW) of the λ 5876 Å HeI line and rotational velocity (standard stars from Sletteback et al. 1975). The solid line is the least square fit given at the top of the figure (cf. Eq. 8). Spectral types and luminosity class of the observed stars are given next to their symbols. HIW errors do not exceed the symbol dimension. For errors in V_{rot} sin$i$ see Sletteback et al. (1975).

5. Rotational Velocities

To estimate the projected rotational velocities of the program stars (V_{rot} sin$i$) we have selected a sample of early type objects from the rotational velocity standards given by Sletteback et al. (1975). We have observed them with the same Echelle+CCD set-up used for BD+00°1617.

Helium lines are notoriously a good choice for rotational velocity determination in early type stars (they are less affected by Stark broadening compared to hydrogen and are stronger than metallic lines). λ 5876 Å is the best recorded helium line in our spectra of BD+00°1617 and the half-intensity width (HIW) of the λ 5876 Å HeI line has been measured on all standard stars. In Figure 7 the HIW of the λ 5876 Å HeI line for the Sletteback et al. (1975) standard stars is plotted against the tabulated rotational velocity. The correction for the instrumental PSF has been applied to the data assuming that the PSF and the rotationally broaden profile (at low V_{rot}) combine as:

$$\sigma^2_{rotation} = \sigma^2_{observed} - \sigma^2_{PSF} \tag{7}$$

The instrumental PSF has been derived from the profile of night-sky emission lines (which follow the same optical path as the stellar light). The effect of the correction is quite small and the induced displacement in Figure 7 is barely noticeable only for the two stars with $V_{rot}\,\sin i\ < 50$ km sec^{-1}.

As expected, a quite straight linear relation exists in Figure 7 between the projected rotational velocity and the HIW, equally valid for main sequence and giant stars. A least square fit gives:

$$V_{rot}\,\sin i\ =\ 42.42 \times HIW\ -\ 35 \qquad km\ sec^{-1} \tag{8}$$

The average HIW of the λ 5876 Å HeI line for the BD+00°1617 stars as measured on all available spectra is given in Table 5 together with the corresponding projected rotational velocity inferred from relation (8).

The low values of $V_{rot}\,\sin i$ for BD+00°1617 stars agree with the high fraction (2/3) of binaries, a general trend first noted by Abt & Hunter (1962 – and confirmed by later investigations, cf. Hack & Struve 1969) who pointed out how tidal energy dissipation in close binaries is expected to act as a breaking mechanism on stellar rotation.

6. Helium lines variability

The equivalent width (EW) and half-intensity width (HIW) of the λ 5876 Å HeI line have been measured on all spectra of the program stars. The individual measures are plotted as function of time in Figures 5 and 6. In Table 5 the dispersion of the measurements, their mean and the error of the mean are given. There is a striking evidence: HeI lines in the two binary stars vary by a large amount both in equivalent width and in broadness while they are remarkably constant in the non-binary #23 star. The amplitude of variation is one order of magnitude the error of the measurements (fixed by the dispersion around the mean for the non-binary #23) and therefore the detection has to be considered as quite robust.

The variation can in principle either be (*a*) intrinsic to the primary, or (*b*) ascribed to the visibility of the spectrum of the secondary blended with the primary's one. The following discussion leads to the conclusion that the variations are most probably intrinsic to the primary.

First, we discuss the possibility that the variations are induced by the visibility of the spectrum of the secondary. Both the EW and HIW of the HeI line vary by a factor of two. Thus the intensity of the HeI line in the companion star should be similar to that of the primary and the two must have similar brightness. From Jasheck & Jaschek (1987) a general upper limit to the *intrinsic* rotational velocity of late O stars may be taken to be V_{rot} ∼300 km sec^{-1}. Comparison with the projected rotational velocity in Table 3 gives a lower limit to the inclination of the rotational axis. The assumption that rotational axis and the orbital axis are roughly aligned puts the constraint on the mass of the companion from the mass function in Table 4. For star #20 this is

$$i^{\#20}_{rot} \simeq i^{\#20}_{orb} \geq 18^\circ \ \longrightarrow\ \left[\frac{M_2^3}{(M_1+M_2)^2}\right]_{\#20} \leq 0.64$$

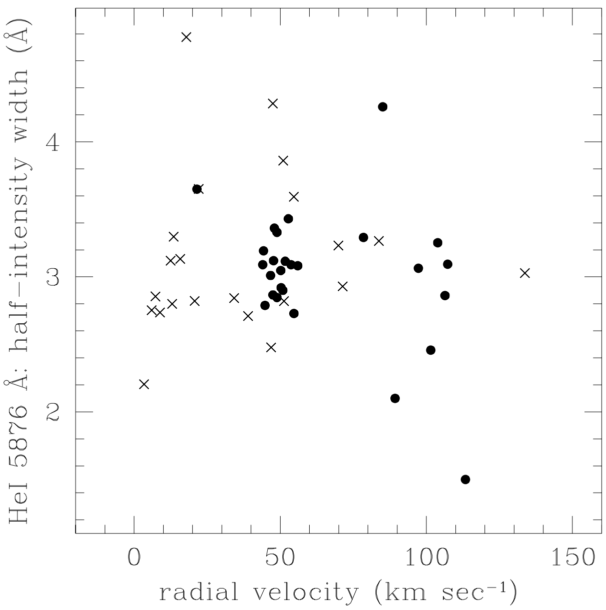

Fig. 8. Half-intensity width (HIW) of HeI 5876 Å plotted against radial velocity for #20 (filled circles) and #21 (crosses). The expected distribution for an unresolved double lined spectroscopic binary is V-shaped, with maximum HIW reached at extrema of the velocity range. This is clearly not the case for both stars which distributions on the graph do not show any correlation with the radial velocity.

$$\longrightarrow\ M_2^{\#20}\ \leq 8\ \ M_\odot \tag{9}$$

The masses are taken as M(O7 V) = 28 $M_\odot$ and M(O9 V) = 19 $M_\odot$ (cf. Conti 1975). This *maximum* mass for the secondary in #20 correspond to a B5 main sequence, which is vastly too dim to rival in brightness and HeI line intensity with the O9 primary. The HeI line variability in #20 therefore cannot be ascribed to the visibility of the companion and it is therefore intrinsic to the primary.

For #21 (an O7 V from Table 1) the situation remains unsettled because the same above line of reasoning on inclination leads to

$$i^{\#21}_{rot} \simeq i^{\#21}_{orb} \geq 19^\circ \ \longrightarrow\ \left[\frac{M_2^3}{(M_1+M_2)^2}\right]_{\#21} \leq 8.4$$
$$\longrightarrow\ M_2^{\#21}\ \leq 31\ \ M_\odot \tag{10}$$

which is compatible with a companion of the same mass and therefore the same brightness.

The most stringent argument on the nature of the HeI line variability comes however from the search of a correlation between extrema in the HeI variation and extrema in the radial velocities. The result is presented in Figure 8. Maximum split between the lines of the primary and secondary (and therefore a maximum HIW value) has to be expected when the primary is passing through radial velocity extrema, resulting in a V-shaped distribution of the points in Figure 8. The latter clearly shows this not to be the case for both #21 and #20, which HeI line variability is intrinsic to the O primary star and appears triggered by the binarity.

Absorption line variability is known to occur in early type stars, both single and binary systems, although no satisfactory explanation yet exists for the phenomenon. Jaschek, Jaschek and Kucewicz (1968) reported that in HD 125823 (B7 III) the HeI lines vary enormously from those of a B2 to those of a B9 star, while all other lines remain constant and photometric and RV variations are *at most* marginal (Norris 1971). We too (Lattanzi, Massone and Munari 1992) identified two helium variable stars (their mean spectra suggesting a classification toward late main sequence B stars) in the young open cluster NGC 225. *Struve–Sahade effect* is termed by Howarth et al. (1997) the systematic variation in relative line strength as a function of orbital phase in double-lined spectroscopic binaries of early types. In their investigation based on IUE spectra the frequency of incidence of such an effect on double-lined OB spectroscopic binaries is 1 in 4. When the effect is present, radial velocity curves appear more "noisy" than expected solely on the base of accuracy of the measurements (cf. Struve 1948 for the template case of the double-lined O8 V spectroscopic binary HD 47129, the Plaskett's star).

7. Galactic rotation

The component of the radial velocity due to the galactic rotation may be written as (cf. Hron 1987):

$$RV_\odot = w_\circ \sin b + u_\circ \cos l \cos b - v_\circ \sin l \cos b - 2[A(R-R_\circ)+\alpha(R-R_\circ)^2] \sin l \cos b \quad (11)$$

where

$$A: \ Oort's\ constant = -\frac{R_\circ}{2}\left(\frac{d\omega}{dR}\right)_{R_\circ}$$

$$\alpha: \ curvature\ term = -\frac{R_\circ}{4}\left(\frac{d^2\omega}{dR^2}\right)_{R_\circ}$$

$$R = \sqrt{R_\circ^2 + d^2 - 2R_\circ d \cos l}$$

and R, $R_\circ$ are the cluster and Sun galacto-centric distances, d the distance cluster–Sun, (l,b) the heliocentric galactic coordinates of the cluster and $(u_\circ, v_\circ, w_\circ)$ is the solar motion vector. Adopting from MC95 a cluster distance of 6 kpc and $(u_\circ, v_\circ, w_\circ)$ = (–9.32,11.18,7.0) km sec^{-1} from Pont et al. (1994), Eq.(11) rewrites as:

$$RV_\odot = 13.8 + 5.8A + 31.8\alpha \quad (12)$$

Hron (1987) has used distances and radial velocities to young open clusters to investigate the rotation curve of the Galaxy. His results (valid for the range $-3 < R - R_\circ < 5$ kpc) are best fitted by $A = 17.0 \pm 1.5$ km sec^{-1} kpc^{-1} and $\alpha = -2.0 \pm 0.6$ km sec^{-1} kpc^{-2}. It has to be noted that Bochum 2 lies at $\sim$14 kpc from the galactic center, therefore outside the limits of applicability for Hron's relations, but taking $\alpha = -1.4$ km sec^{-1} kpc^{-2} (inside the quote errors) Eq.(12) gives a radial velocity of +68 km sec^{-1}, coincident with the observed value for Bochum 2 (cf. Eq. 6).

Acknowledgments

We would like to express our gratitude to G. Carraro and T. Zwitter who helped to secured the spectra on Dec 16, 1994 and Jan 15, 1995, to R. Barbon and G. Carraro for useful discussions and to R. Passuello for his expert assistance with Linux/IRAF.

References

Abt H. A., Hunter J. H. jr., 1962, ApJ 136, 381
Ambartsumian V. A., 1954, Comm. Byurakan Obs. 15, 3
Conti P. S., 1975, in *HII regions and related topics*, T. L. Wilson and D. Downes ed.s, Springer-Verlag, p. 207
Jackson P. D., Fitzgerlad M. P., Moffat A. F. J., 1979, in IAU Symp. 84 *The large scale characteristics of the Galaxy* W. B. Burton ed., Reidel, p. 221
Jaschek M., Jaschek C., Kucewicz B., 1968, Nature 225, 246
Jaschek C., Jaschek M., 1987, The classification of stars, Cambridge Univ. Press
Jeffers, H. M., van den Boss, W. H., Creeby, F. M., 1963, Index Catalogue of visual Double Stars, Publ. Lick Obs. 21
Hack M., Struve O., 1969, Stellar Spectroscopy, Astronomical Observatory of Trieste
Halbwachs J. L., Bessgeng G., Bastian U., Egret D., Hog E., Van Leeuwen F., Petersen C., Schwekendiek P., Wicenec A., 1994, A&A 281, 25
Howarth I. D., Seibert K. W., Hussain G. A. J., Prinja R. K., 1997, MNRAS 284, 265
Hron J., 1987, A&A 176, 34
Lasker B. M., Sturch C. R., McLean B. J., Russell J. L., Jenkner H., Shara M. M., 1990, AJ 99, 2019
Lattanzi M. G., Massone G., Munari U., 1991, AJ 102, 177
Moffat A. F. J., Vogt N., 1975, A&AS 20, 85
Moore C. E., 1959, A Multiple Table of Astrophysical Interest, US Dept. of Commerce
Munari U., Zwitter T., 1994, Padova and Asiago Obs. Tech. Rep. 4
Munari U., Carraro G., 1995, MNRAS 277, 1269
Munari U., Lattanzi M. G., 1992, PASP 104, 121
Norris J., 1971, ApJS 23, 235
Pont F., Mayor M., Burki G., 1994, A&A 285, 415
Salukvadze G. N., 1978, Byull. Abastumanskaya Astrofiz. Obs. 49, 39
Sletteback A., Collins II G. W., Boyce P. B., White N. M., Parkinson T. D., 1975 ApJS 29, 137
Struve O., 1948, ApJ 107, 327
Turbide L., Moffat A. F. J., 1993, AJ 105, 1831
Urban S. E., Corbin T. E., 1994, in *Galactic and Solar System Optical Astrometry*, ed. Morrison and Gilmore, Camb. Univ. Press, p.11
Urban S. E., Corbin T. E., 1996, A&A 305, 989
Zacharias N., Zacharias M. I., Douglass G. G., Wycoff G. L., 1996, AJ 112, 2336

This article was processed by the author using Springer-Verlag LaTeX A&A style file *L-AA* version 3.